Axion Radiation from Strings

C. Hagmann[1], S. Chang[2] and P. Sikivie[3]

[1]*Lawrence Livermore National Laboratory, Livermore, CA 94550*
[2]*Department of Physics, Purdue University, W. Lafayette, IN 47907*
[3]*Department of Physics, University of Florida, Gainesville, FL 32611*
(February 1, 2008)

Abstract

This paper revisits the problem of the string decay contribution to the axion cosmological energy density. We show that this contribution is proportional to the average relative increase when axion strings decay of a certain quantity N_{ax} which we define. We carry out numerical simulations of the evolution and decay of circular and non-circular string loops, of bent strings with ends held fixed, and of vortex-antivortex pairs in two dimensions. In the case of string loops and of vortex-antivortex pairs, N_{ax} decreases by approximately 20%. In the case of bent strings, N_{ax} remains constant or increases slightly. Our results imply that the string decay contribution to the axion energy density is of the same order of magnitude as the well-understood contribution from vacuum realignment.

I. INTRODUCTION

The axion was proposed over two decades ago as a solution to the 'Strong CP Problem', i.e. to explain why QCD conserves the discrete symmetries P and CP in spite of the fact that the Standard Model as a whole violates those symmetries. It is the quasi-Nambu-Goldstone boson [1] associated with the spontaneous breakdown of a $U_{PQ}(1)$ symmetry which Peccei and Quinn postulated [2]. The properties of the axion depend mainly on one unknown parameter, the magnitude of the vacuum expectation value v_a which breaks $U_{PQ}(1)$. The mass of the axion and its couplings are inversely proportional to v_a. The (zero-temperature) mass is given by:

$$m_a \simeq 6 \ \mu\text{eV} \ \cdot N \cdot \frac{10^{12}\text{GeV}}{v_a} \quad . \tag{1.1}$$

N is a strictly positive integer that describes the color anomaly of $U_{PQ}(1)$. The combination of parameters $f_a \equiv \frac{v_a}{N}$ is usually called the "axion decay constant".

A priori v_a, and therefore m_a, is a free parameter of the theory. However, it is severely constrained by accelerator experiments and astrophysical arguments. Combined, the accelerator and astrophysical constraints imply $m_a \lesssim 10^{-2}\text{eV}$ [3]. In addition, there is a *lower* limit on the axion mass from the requirement that axions do not overclose the Universe. The axion cosmological energy density receives contributions from vacuum realignment [4], from string decay [5–11], and from wall decay [8,12–14]. All three contributions increase with decreasing axion mass. The contribution whose size has been most controversial, and which is the topic of this paper, is that from string decay.

Axion models contain strings because they have a spontaneously broken U(1) symmetry, namely $U_{PQ}(1)$. The latter is a global symmetry and hence axion strings are *global* strings. The strings are only present when the axion is massless, but such is indeed the case in the very early universe, when the temperature is much larger than 1 GeV. For the purposes of this paper we may describe the dynamics of axions and axion strings by the action density:

$$\mathcal{L} = \frac{1}{2}\partial_\mu \phi^\dagger \partial^\mu \phi - \frac{\lambda}{4}(\phi^\dagger \phi - v_a^2)^2 \quad , \tag{1.2}$$

where $\phi \equiv \phi_1 + i\phi_2$ is a complex scalar field. $\mathcal{L}$ is invariant under the $U_{PQ}(1)$ symmetry: $\phi \to e^{i\alpha}\phi$. The symmetry is spontaneously broken by the vacuum expectation value

$$\phi = v_a \ e^{i\frac{a}{v_a}} \tag{1.3}$$

where a is the axion field. A static axion string stretched along the z axis is the field configuration:

$$\phi = v_a \ f(\frac{r}{\delta}) \ e^{i\theta} \quad , \tag{1.4}$$

where (z, r, θ) are cylindrical coordinates, $\delta \equiv \frac{1}{\sqrt{\lambda}v_a}$ is the string core size, and $f(\frac{r}{\delta})$ is a function which goes to zero when $r \to 0$, approaches one for $r \gg \delta$, and solves equations of motion which follow from Eq. (1.2). The energy per unit length of the string is

$$\tau = \int d^2x \, [\frac{1}{2}|\vec{\nabla}\phi|^2 + \frac{\lambda}{4}(\phi^\dagger\phi - v_a^2)^2]$$

$$\simeq \int_{\rho>\delta} d^2x \, \frac{v_a^2}{2} \, |\vec{\nabla}e^{i\theta}|^2 = \pi v_a^2 \ln(\frac{L}{\delta}) \tag{1.5}$$

where L is an infra-red cutoff. The R.H.S. of Eq.(1.5) neglects the contribution to τ from the string core. The string core contribution is of order πv_a^2, i.e. it is smaller than the contribution (1.5) of the field outside the string core by the factor $\ln(L/\delta)$. In the situations of interest to us, $\ln(\frac{L}{\delta}) \simeq 67$. Indeed, for axion strings in the early universe, the infra-red cutoff is provided by the presence of neighboring strings. L is then of order the distance between strings which, as we will see, is of order the horizon scale. The relevant time is the start of the QCD phase transition, and hence $L \sim 10^{-7}$ sec. On the other hand, $\delta^{-1} \sim v_a \sim 10^{12}$ GeV.

Eq. (1.5) is valid for many but not all axion models. In general

$$\tau \simeq \pi(\frac{v_a}{K})^2 \ln(\frac{L}{\delta}) \tag{1.6}$$

where K is a model-dependent integer defined as follows. Let α be the angle conjugate to the PQ charge. K is the factor by which the period in α of the manifold of vacuum expectation values of the model is reduced by the presence of exact continuous symmetry transformations, such as gauge transformations. In the PQWW model [2,1] $K = 2$, whereas in the DFSZ [15] and KSVZ [16] models $K = 1$.

Axion strings appear as topological defects in the early universe when $U_{PQ}(1)$ becomes spontaneously broken by the vacuum expectation value (1.3), at a temperature of order v_a. The phase transition where this happens is called the PQ phase transition. We assume in this paper that no inflation occurs after the PQ phase transition. If there is inflation after the PQ transition, the axion field gets homogenized over enormous distances and the axion strings are 'blown away'. In that case there is no string, nor wall, decay contribution to the axion cosmological energy density.

At first the strings are stuck in the plasma [6], but soon the plasma becomes sufficiently dilute that the strings move freely and acquire relativistic speeds. The strings are present till the axion mass turns on at the QCD phase transition. The critical time is t_1 defined by $m_a(T(t_1))t_1 = 1$, where $m_a(T)$ is the temperature-dependent axion mass. One finds [4]

$$t_1 \simeq 2 \cdot 10^{-7} \text{sec} \left(\frac{f_a}{10^{12}\text{GeV}} \right)^{\frac{1}{3}} . \tag{1.7}$$

The corresponding temperature is:

$$T_1 \simeq 1\text{GeV} \left(\frac{10^{12}\text{GeV}}{f_a} \right)^{\frac{1}{6}} . \tag{1.8}$$

All strings become the edges of N_d domain walls at t_1, where N_d is the number of degenerate vacua of the axion model [17]. It is related to N by

$$N_d = \frac{N}{K} \tag{1.9}$$

3

where K is the same factor as appears in Eq.(1.6). If $N_d \geq 2$, the universe becomes domain wall dominated. The resulting cosmology is inconsistent with observation. If $N_d = 1$, the walls bounded by string are unstable and decay into axions [18]. We recently gave a detailed discussion of the wall decay contribution to the axion cosmological energy density [14].

In this paper, our goal is to determine the present energy density $\rho_a^{\text{str}}(t_0)$ in axions that were radiated by axions strings between the PQ phase transition and time t_1. In section 2, we analyse the problem theoretically. We express $\rho_a^{\text{str}}(t_0)$ in terms of quantities ξ, χ and $\bar{r}$ which parametrize the main sources of uncertainty. Most of the past debate has focused on $\bar{r}$ which is a functional of the energy spectrum of axions emitted by strings. The remaining sections of the paper report on our estimates of $\bar{r}$ using numerical simulations. Section 3 describes our simulations of the motion and decay of circular and non-circular string loops. Section 4 does the same for bent strings. Section 5 describes our simulations of the motion and annihilation of vortex-antivortex pairs in 2 (space) dimensions. The behaviour of the vortex-antivortex system can be predicted by analytical methods in the regime where the vortex and antivortex do not overlap. Thus the vortex-antivortex pair provides an interesting case study where theory and simulation can be confronted with each other. In section 6 we summarize our results and compare them to the previous simulations by two of us [8], to those of Battye and Shellard [9], and those of Yamaguchi, Kawasaki and Yokoyama [11].

II. THEORETICAL ANALYSIS

As we shall see, the axions radiated by strings become non-relativistic soon after t_1. Since each axion contributes m_a to the energy today, our focus is on determining their *number* density $n_a^{\text{str}}(t)$.

Axions are radiated by collapsing string loops and by oscillating wiggles on long strings. By definition, long strings stretch across the horizon. They move at relativistic speeds and intersect one another. When strings intersect, there is a high probability of reconnection, i.e. of rerouting of the topological flux [19]. Because of such 'intercommuting', long strings produce loops which then collapse freely. In view of this efficient decay mechanism, the average density of long strings is expected to be of order the minimum consistent with causality, namely one long string per horizon. Hence the energy density in long strings:

$$\rho_{\text{str}}(t) = \xi \frac{\tau}{t^2} \simeq \xi \pi (\frac{v_a}{K})^2 \frac{1}{t^2} \ln(\frac{t}{\delta}) \quad , \tag{2.1}$$

where ξ is a parameter of order one.

The equations governing the number density $n_a^{\text{str}}(t)$ of axions radiated by axion strings are [6]

$$\frac{d\rho_{\text{str}}}{dt} = -2H\rho_{\text{str}} - \frac{d\rho_{\text{str} \to a}}{dt} \tag{2.2}$$

and

$$\frac{dn_a^{\text{str}}}{dt} = -3Hn_a^{\text{str}} + \frac{1}{\omega(t)} \frac{d\rho_{\text{str} \to a}}{dt} \tag{2.3}$$

where $\omega(t)$ is defined by:

$$\frac{1}{\omega(t)} = \frac{1}{\frac{d\rho_{\text{str}\to a}}{dt}} \int \frac{dk}{k} \frac{d\rho_{\text{str}\to a}}{dt\, dk} \quad . \tag{2.4}$$

k is wavevector magnitude. $\frac{d\rho_{\text{str}\to a}}{dt}(t)$ is the rate at which energy density gets converted from strings to axions at time t, and $\frac{d\rho_{\text{str}\to a}}{dt\, dk}(t,k)$ is the spectrum of the axions produced. $\omega(t)$ is therefore the average energy of axions radiated in string decay processes at time t. The term $-2H\rho_{\text{str}} = +H\rho_{\text{str}} - 3H\rho_{\text{str}}$ in Eq. (2.2) takes account of the fact that the Hubble expansion both stretches $(+H\rho_{\text{str}})$ and dilutes $(-3H\rho_{\text{str}})$ long strings. Integrating Eqs. (2.1 - 2.3), setting $H = \frac{1}{2t}$, and neglecting terms of order one versus terms of order $\ln(\frac{t}{\delta})$, one obtains

$$n_a^{\text{str}}(t) \simeq \frac{\xi\pi v_a^2}{K^2 t^{\frac{3}{2}}} \int_{t_{\text{PQ}}}^t dt' \frac{\ln(\frac{t'}{\delta})}{t'^{\frac{3}{2}}\omega(t')} \quad , \tag{2.5}$$

where t_{PQ} is the time of the PQ transition.

The central question is: what is the average energy $\omega(t)$ of axions radiated in string decay processes at time t? Axions are radiated by wiggles on long strings and by collapsing string loops. Consider a process which starts at t_{in} and ends at t_{fin}, and which converts an amount of energy E from string to axions. t_{in} and t_{fin} are both of order t. The number of axions radiated is

$$N = \int dk \frac{dE}{dk}(t_{\text{fin}})\frac{1}{k} \tag{2.6}$$

where $\frac{dE}{dk}(t_{\text{fin}})$ is the energy spectrum of the ϕ field in the final state. The average energy of axions emitted is:

$$\omega = \frac{E}{N} \quad . \tag{2.7}$$

It is useful to define the quantity [8]

$$N_{\text{ax}}(t) \equiv \int dk \frac{dE}{dk}(t)\frac{1}{k} \quad . \tag{2.8}$$

The final value of N_{ax} is N. The initial value of N_{ax} is determined in terms of E by the fact that the energy stored in string has spectrum $\frac{dE}{dk}(t_{\text{in}}) \sim \frac{1}{k}$. This spectral shape - equal energy per unit logarithmic wavevector interval - is implied by Eq. (1.5). If $\ell \equiv \frac{E}{\tau}$ is the length of string converted to axions, we have

$$\frac{dE}{dk}(t_{\text{in}}) = \pi(\frac{v_a}{K})^2 \ell \frac{1}{k} \tag{2.9}$$

for $k_{\text{min}} < k < k_{\text{max}}$ where k_{max} is of order $\frac{2\pi}{\delta}$ and k_{min} of order $\frac{2\pi}{t}$. t plays the role of L in Eq. (1.5). Hence

$$N_{\text{ax}}(t_{\text{in}}) = \pi(\frac{v_a}{K})^2 \ell \int_{k_{\text{min}}}^{\delta^{-1}} dk \frac{1}{k^2} = \frac{E}{\ln(\frac{t}{\delta})k_{\text{min}}} \tag{2.10}$$

Combining Eqs. (2.6 - 2.10) yields

5

$$\frac{1}{\omega} = \frac{r}{\ln(\frac{t}{\delta})k_{\min}} \tag{2.11}$$

where r is the relative change in $N_{\text{ax}}(t)$ during the process in question:

$$r \equiv \frac{N_{\text{ax}}(t_{\text{fin}})}{N_{\text{ax}}(t_{\text{in}})} \quad . \tag{2.12}$$

$k_{\min}$ is of order $\frac{2\pi}{L}$ where L is the loop size in the case of collapsing loops, and the wiggle wavelength in the case of bent strings. L is at most of order t but may be substantially smaller than that if the string network has a lot of small scale structure. To parametrize our ignorance in this matter, we define χ such that the suitably averaged $k_{\min} = \chi \frac{2\pi}{t}$. Combining Eqs. (2.5) and (2.11) we find:

$$n_a^{\text{str}}(t) \simeq \frac{\xi \bar{r}}{\chi} \frac{v_a^2}{K^2 t} \quad , \tag{2.13}$$

where $\bar{r}$ is the weighted average of r over the various processes that convert string to axions.

Let us show that the set of all axions that were radiated between t_{PQ} and t have spectrum $\frac{dn_a}{dk} \sim \frac{1}{k^2}$ for $\frac{1}{t} \lesssim k \lesssim \frac{1}{\sqrt{tt_{\text{PQ}}}}$, irrespective of the shape of $\frac{d\rho_{\text{str}\to a}}{dt\,dk}$. Indeed scaling implies

$$\frac{d\rho_{\text{str}\to a}}{dt\,dk}(t,k) = \frac{d\rho_{\text{str}\to a}}{dt}(t)f(tk)t \ , \tag{2.14}$$

where the unknown function $f(u)$ is normalized such that

$$\int_0^\infty f(u)du = 1 \ . \tag{2.15}$$

We will only assume that $f(u)$ has appreciable support near $u = 1$. Eqs. (2.1, 2.2) imply

$$\frac{d\rho_{\text{str}\to a}}{dt}(t) \simeq \frac{1}{t}\rho_{\text{str}}(t) \quad , \tag{2.16}$$

where "$\simeq$" indicates, as before, that terms of order one are neglected versus terms of order $\ln(\frac{t}{\delta})$. Since axions free-stream after they are emitted, and $R \sim \sqrt{t}$ at the relevant epoch, we have:

$$\frac{dn_a}{dk}(t,k) = \int_{t_{\text{PQ}}}^t dt' \frac{d\rho_{\text{str}\to a}}{dt\,dk}(k',t') \frac{1}{k'} \left(\frac{t'}{t}\right) \tag{2.17}$$

with $k' = k(\frac{t}{t'})^{\frac{1}{2}}$. The factor $\frac{t'}{t}$ accounts for the redshift and the volume expansion between t' and t. Using Eqs. (2.14, 2.16) and (2.1), one obtains

$$\frac{dn_a}{dk}(t,k) \simeq \frac{\xi \pi (\frac{v_a}{K})^2}{k^2 t^2} \int_{k\sqrt{tt_{\text{PQ}}}}^{kt} du f(u) \ln(\frac{u^2}{k^2 t\delta}) \quad . \tag{2.18}$$

For $\frac{1}{t} \lesssim k \lesssim \frac{1}{\sqrt{tt_{\text{PQ}}}}$, the integral in Eq. (2.18) is only a slowly varying function of k compared to the factor $\frac{1}{k^2}$. That is the promised result.

Since their momenta are of order t_1^{-1} at time t_1, the axions become non-relativistic soon after they acquire mass. Therefore, the string decay contribution to the axion energy density today is

$$\rho_a^{\text{str}}(t_0) = m_a n_a^{\text{str}}(t_1)(\frac{R_1}{R_0})^3 \simeq m_a \frac{\xi \bar{r}}{\chi} \frac{v_a^2}{K^2 t_1}(\frac{R_1}{R_0})^3 \tag{2.19}$$

where $\frac{R_1}{R_0}$ is the ratio of scale factors between t_1 and today. For comparison, the contribution from vacuum realignment is [4]

$$\rho_a^{\text{vac}}(t_0) \simeq m_a \frac{f_a^2}{t_1}(\frac{R_1}{R_0})^3 \quad . \tag{2.20}$$

In terms of the critical energy density $\rho_c = \frac{3H_0^2}{8\pi G}$, the vacuum realignment contribution is:

$$\Omega_a^{\text{vac}} \equiv \frac{\rho_a^{\text{vac}}(t_0)}{\rho_c} \simeq \frac{1}{3}(\frac{f_a}{10^{12}\text{GeV}})^{\frac{7}{6}}(\frac{0.7}{h})^2 \quad . \tag{2.21}$$

As usual, h parametrizes the present Hubble rate $H_0 = h \cdot 100 \frac{\text{km}}{\text{sec}\cdot\text{Mpc}}$. The contribution from wall decay is [14]

$$\rho_a^{\text{d.w.}}(t_0) \simeq m_a \frac{6}{\gamma} \frac{f_a^2}{t_1}(\frac{R_1}{R_0})^3 \tag{2.22}$$

where γ is the average Lorentz factor of axions produced in the decay of walls bounded by string. In simulations, we found $\gamma \sim 7$ for $\frac{v_a}{m_a} \simeq 500$, but that γ increases approximately linearly with $\ln(\frac{v_a}{m_a})$. Extrapolation of this behaviour to the parameter range of interest, $\ln(\frac{v_a}{m_a}) \simeq 60$, yields $\gamma \sim 60$. It suggests that the wall decay contribution is subdominant relative to the vacuum realignment contribution.

The ratio of the string decay and vacuum realignment contributions is:

$$\frac{\rho_a^{\text{str}}(t_0)}{\rho_a^{\text{vac}}(t_0)} \simeq \frac{\xi \bar{r} N_d^2}{\chi} \quad . \tag{2.23}$$

where we used Eq. (1.9). Each of the factors on the R.H.S. deserves discussion:

N_d Almost surely one needs $N_d = 1$ to avoid the cosmological disaster of an axion domain wall dominated universe. It may be worth pointing out, however, that the domain wall problem can be avoided, in $N_d > 1$ models, by introducing an interaction which slightly lowers one of the N_d vacua with respect to the others [17]. The lowest vacuum takes over after some time and the walls disappear before they dominate the energy density. There is little room in parameter space for this to happen, but it is logically possible. It is discussed in detail in ref. [14].

ξ In previous work [8,10], we set $\xi = 1$ on the argument that the number density of long strings should be close to the minimum consistent with causality, i.e. of order one long string per horizon. Battye and Shellard [9] set $\xi \simeq 13$ because this describes the density of strings in simulations of *local* string networks in an expanding universe. However, axion strings are *global* strings. Unlike global strings, local strings have all their energy located in the string core. Also, they cannot dissipate their energy by emitting Nambu-Goldstone radiation as

global strings do. For these reasons, it is not obvious that global strings are as dense in the early universe as local strings would be. In fact, M. Yamaguchi, M. Kawasaki and J. Yokoyama [11] have done simulations of global string networks in an expanding universe and find $\xi \simeq 1$.

χ χ and ξ are related since the average interstring distance controls both. On dimensional grounds, $\chi \sim \sqrt{\xi}$. So, the effect of small scale structure in the axion string network partially cancels out in the RHS of Eq. (2.19). In previous work [8,10], we have assumed $\chi \simeq 1$ but this could be off by a factor two or so.

$\bar{r}$ This is the unknown on which most of the past debate has focused. Two basic scenarios have been put forth, which we call A and B. The question is: what is the spectrum of axions radiated by strings? The main source is closed loops of size $L \sim t$. Scenario A postulates that a bent string or closed loop oscillates many times, with period of order L, before it has released its excess energy and that the spectrum of radiated axions is concentrated near $\frac{2\pi}{L}$. In that case one has $\bar{r} \sim \ln(\frac{t_1}{\delta}) \simeq 67$. Scenario B postulates that the bent string or closed loop releases its excess energy very quickly and that the spectrum of radiated axions is $\frac{dE}{dk} \sim \frac{1}{k}$ with a high frequency cutoff of order $\frac{2\pi}{\delta}$ and a low frequency cutoff of order $\frac{2\pi}{L}$. In scenario B, the initial and final spectra $\frac{dE}{dk}$ of the energy stored in the axion field are qualitatively the same and hence $\bar{r} \sim 1$. In scenario A, the string decay contribution dominates over the vacuum realignment contribution by the factor $\ln(\frac{t_1}{\delta})$, whereas, in scenario B, the contributions from string decay and vacuum realignment have the same order of magnitude.

Computer simulations offer a way to try and estimate $\bar{r}$. It should be kept in mind however that present day technology limits lattice sizes to approximately 256^3 in 3 dimensions (3D), and 4096^2 in 2D. Hence the ratio of loop/core size that can be investigated is limited to $\ln(\frac{L}{\delta}) \simeq 3.5$ in 3D, and 5 in 2D, whereas $\ln(\frac{L}{\delta}) \simeq 67$ in the situations of physical interest. It is therefore important to investigate the dependence, if any, of the results of computer simulations on $\ln(\frac{L}{\delta})$ over the small range that can be investigated. The following three sections report on our simulations of circular and non-circular string loops, bent strings, and vortex-antivortex pairs.

III. STRING LOOP SIMULATIONS

We simulated the motion and decay of circular loops initially at rest, and of non-circular loops with angular momentum. The initial configurations are set up on large ($\sim 10^7$ points) Cartesian grids, and time-evolved using the finite-difference equations derived from Eq. (1.2). FFT spectrum analysis of the kinetic and gradient energies during the collapse yields $N_{\text{ax}}(t)$, and hence r.

A. Circular Loops

Because of azimuthal symmetry, circular loops can be studied in $\rho - z$ space. The z-axis is perpendicular to the plane of the loop. By mirror symmetry, the problem can be further reduced to one quarter-plane. The static axion field outside the string core is [8]

$$a(\rho, z) = \frac{v_a}{2}\Omega(\rho, z) \tag{3.1}$$

in the infinite volume limit, where Ω is the solid angle subtended by the loop. We use as initial configuration the outcome of a relaxation routine starting with Eq.(3.1) outside the core and

$$\phi(r) = \tanh(0.58\frac{r}{\delta})e^{i\theta} \tag{3.2}$$

within the core. Here, r is the distance to the string center, and θ is the polar angle about the string. The configuration inside the core is held fixed during the relaxation. The relaxation and subsequent dynamical evolution are done with reflective Neumann-type boundary conditions. A step size $dt = 0.2$ was used for the time evolution. The total energy was conserved to better than 1%.

We call R_0 the initial loop radius. Fig. 1 shows $R(t)$ for collapsing loops. While they collapse, the loops reach speeds close to the speed of light. Figs. 2a through 2e show successive snapshots of the string core as it speeds toward the origin. It is increasingly Lorentz contracted. A lattice effect is observed when the Lorentz contracted core size becomes comparable to the lattice spacing. This effect consists of a "scraping" of the string core on the underlying grid, with dissipation of the kinetic energy of the string into high frequency axion radiation. We chose λ small enough to avoid this phenomenon. For the large ($R_0 = 2400$) 2D circular loop simulations, $\lambda \lesssim 0.01$ is required.

In most cases, the loops collapse without rebound. However, for the range of parameters $80 \lesssim R_0/\delta \lesssim 190$, a bounce occurs. It is shown in Fig. 1 (solid line) for the case $R_0 = 2400$ and $\delta = 15.8$. Figs. 2f through 2l show snapshots of the axion field configuration during the bounce. Note that the orientation of the string switches during the bounce, i.e. a left-oriented loop bounces into a right-oriented one, or vice-versa.

Spectrum analysis of the fields was performed by expanding the gradient plus kinetic energy

$$E_{\text{kin+grad}} = \int_{-L_Z}^{L_z} dz \int_0^{L_\rho} 2\pi\rho d\rho \; (\frac{1}{2}\dot{\phi}^\dagger\dot{\phi} + \frac{1}{2}\vec{\nabla}\phi^\dagger \cdot \vec{\nabla}\phi) \tag{3.3}$$

using

$$\dot{\phi} = \sum_{mn} a_{mn}J_0(k_m\rho)\,\cos(k_n(z + L_z))$$

$$\nabla_z\phi = \sum_{mn} b_{mn}J_0(k_m\rho)\,\sin(k_n(z + L_z))$$

$$\nabla_\rho\phi = \sum_{mn} c_{mn}J_0(k_m\rho)\,\cos(k_n(z + L_z)) \tag{3.4}$$

where the k_m and k_n satisfy $J_0(k_mL_\rho) = 0$ and $\sin(2k_nL_z) = 0$ respectively. The wavevector magnitude of mode (m, n) is $k_{mn} \equiv \sqrt{k_m^2 + k_n^2}$. Fig. 3 shows the power spectrum at $t = 0$ and, after the collapse, at $t = 3000$. At both times, it exhibits an almost flat plateau, consistent with $dE/dk \propto 1/k$. The high frequency cutoff of the spectrum is increased however at the later time, as might be expected since the core gets Lorentz contracted during the collapse. The evolution of $N_{\text{ax}} = \sum_{mn} \frac{E_{mn}}{k_{mn}}$ was studied for various values of R_0/δ.

As shown in Fig. 4, we observe a marked decrease of N_{ax} during the collapse, of order 20% independent of R_0/δ in the investigated range $3.6 \leq \ln(R_0/\delta) \leq 5.0$. In the previous circular loop simulations by two of us [8], in which $\ln(R_0/\delta)$ ranges from 2.5 to 3.4, it was also found that $r \simeq 0.8$.

B. Non-circular loops

Circular loops are a special case and their behaviour may be untypical of loops in general. To address this concern, we performed simulations of non-circular loops as well. The initial condition of the loop is given by its initial position $\vec{r}(s, t_0)$ and velocity $\vec{v}(s, t_0)$, where s parametrizes distance along the loop. Only the transverse part of $\vec{v}(s, t_0)$ has physical meaning. We determine the initial axion field using

$$a(\vec{x}, t_0) = \frac{v_a}{2} \Omega(\vec{x})\{\vec{r}(s, t_0)\} \tag{3.5}$$

where $\Omega(\vec{x})\{\vec{r}(s, t_0)\}$ is the solid angle subtended by the loop as seen from $\vec{x}$. The axion field $a(\vec{x}, t_0 + dt)$ a short time dt later is similarly determined by calculating the solid angle subtended by the loop located at $\vec{r}(s, t_0) + dt\, \vec{v}(s, t_0)$. This yields the initial time derivative of the axion field $\dot{a}(\vec{x}, t_0)$.

Scenario A postulates that an axion string behaves like a Nambu-Goto (NG) string to lowest order in a perturbative expansion in powers of $\frac{1}{\ln(\frac{L}{\delta})}$ where L is the string size. The most general solution to the NG equations of motion is [20]:

$$\vec{r}(s, t) = \frac{R_0}{2}[\vec{a}(\sigma_-) + \vec{b}(\sigma_+)] \tag{3.6}$$

where $\sigma_\pm \equiv (s \pm t)/R_0$, s is proportional to the energy in the string between the points labeled s and $s = 0$, and $\vec{a}(\sigma)$ and $\vec{b}(\sigma)$ are arbitrary functions of period 2π, which satisfy $\vec{a}'(\sigma)^2 = \vec{b}'(\sigma)^2 = 1$. $L = 2\pi R_0$ is the total proper length of the string loop, i.e. $\vec{r}(s + L, t) = \vec{r}(s, t)$. It can be shown [21] that a NG string loop of length L has a motion which is periodic in time with period $L/2$, and that an initially static NG string loop collapses to a doubled-up line after half a period.

A considerable literature [21–24] is devoted to the problem of finding non-intersecting NG loop solutions. The authors are mainly motivated by issues related to the cosmic string scenario of large scale structure formation. However, self-intersection of string loops is also relevant to the question whether scenario A or B is more likely to be correct. Intercommuting (self-intersection with reconnection) favors scenario B because it causes loop sizes to shrink, and hence the average energy of radiated axions to increase. As discussed in Ref. [8], if the probability p of intercommuting per oscillation is larger than of order $\frac{1}{\ln(\frac{L}{\delta})} \simeq 1.4\%$, the spectrum of axions radiated by the original loop, its two daughters, four grand-daughters, and so on, will be qualitatively the same as in scenario B, independently of assumptions on the spectrum of radiation from any single loop.

A particular two-parameter set of solutions [21,22] is given by:

$$x(s, t) = \frac{R_0}{2}\left((1 - \alpha)\sin\sigma_- + \frac{1}{3}\alpha\sin 3\sigma_- + \sin\sigma_+\right)$$

10

$$y(s,t) = \frac{R_0}{2}\left(-(1-\alpha)\cos\sigma_- - \frac{1}{3}\alpha\cos 3\sigma_- - \cos\psi\cos\sigma_+\right)$$
$$z(s,t) = \frac{R_0}{2}\left(-2\sqrt{\alpha(1-\alpha)}\cos\sigma_- - \sin\psi\cos\sigma_+\right) \quad . \tag{3.7}$$

with $\alpha \in (0,1)$ and $\psi \in (-\pi, \pi)$. In a large region of (α, ψ) parameter space, the loop does not self-intersect [24].

We performed 21 simulations of non-circular loops using Eqs.(3.7) as initial conditions, on a 256^3 lattice with periodic boundary conditions. Each simulation took approximately 1 week to run. A variety of (α, ψ) and λ values were chosen. Figure 5 shows the collapse of a non-circular loop projected onto the xz plane. Here, and in all cases tried, the loop size shrinks to zero in one go, without oscillation or rebound. Standard Fourier techniques were used for the spectrum analysis, and N_{ax} was computed as a function of time. In all but two of the cases tried, N_{ax} decreases while the loop collapses. The r values depend upon α, ψ and λ, and cover the range 0.6 to 1.07. Figure 6 shows $N_{\text{ax}}(t)$ for $R_0 = 72, \alpha = 0.7, \psi = \pi/2$ and $\lambda = 0.0125, 0.025, 0.05$ and 0.1. Some of the largest r values (1.06, 0.94, 0.90 and 0.89 respectively) were obtained in these simulations. In them, and in all cases where $\ln(\frac{R_0}{\delta})$-dependence was tested, r decreases with increasing $\ln(\frac{R_0}{\delta})$. It appears however that the second derivative is decreasing and that r may reach an asymptotic value for $\ln(\frac{R_0}{\delta}) \sim 3$. For $\alpha = 0.7$, $\psi = \pi/2$, the asymptotic value would be of order 0.9.

Nine simulations were done for $\lambda = 0.05$ and $R_0 = 72$ (hence $\ln(\frac{R_0}{\delta}) = 2.78$) and a variety of (α, ψ) values. The average of r over this set is 0.77.

IV. BENT STRING SIMULATIONS

We have also carried out simulations of oscillating bent strings with ends held fixed. The oscillation amplitude decreases as the string loses energy to axion radiation. We choose the z axis parallel to the direction of the string when straight. $L_x L_y L_z$ is the size of the box. Initial configurations describing static, sinusoidally shaped strings were prepared using the ansatz

$$\phi(x,y,z) = \tanh(\frac{.58\,r}{\delta})\,\exp\left(i\arctan\left(\frac{y-y_0}{x-x_0-A_0\sin(\frac{2\pi z}{\Lambda})}\right)\right) \tag{4.1}$$

where $r = \sqrt{(x-x_0-A_0\sin(\frac{2\pi z}{\Lambda}))^2 + (y-y_0)^2}$, A_0 is the initial amplitude, $(x_0, y_0) = (\frac{L_x}{2}, \frac{L_y}{2})$ is the equilibrium position of the string and $\Lambda = L_z$ is the string wavelength. We used square boxes ($L_x = L_y$) in all cases.

The field outside the core was thoroughly relaxed before dynamical time evolution was begun. Neumann boundary conditions were imposed on the four side faces ($x = 0, L_x$, and $y = 0, L_y$) and periodic boundary conditions on the endfaces ($z = 0, L_z$). The kinetic + gradient energy in the ϕ field was spectrum analyzed at regular time intervals during the dynamical evolution. We took care to avoid finite volume and discrete space-time effects. To minimize finite volume (i.e. boundary) effects, $L_x, L_y \geq 4L_z$ is needed. To avoid discretization effects, $\lambda \leq 0.4$ and time step $dt \leq 0.2$ are needed. When the latter conditions are satisfied, no scraping of the string on the underlying lattice is observed and total energy is conserved to better than one part in 10^3.

We performed runs for a variety of box sizes, initial amplitudes A_0 and core sizes $\delta = \frac{1}{\sqrt{\lambda}}$. Fig. 7 shows the amplitude $A(t)$ as a function of time for initial amplitudes $A_0 = 20$ and 10, on a 256*256*64 lattice and $\lambda = 0.2$. For $t \lesssim 250$, the damped oscillator behaviour of $A(t)$ is very smooth and regular. For $t \gtrsim 250$, $A(t)$ is less regular because the string is being driven by radiation which was emitted in the first couple of oscillations and which returned to the string's location after reflection by the sidewalls,

Fig. 7 shows that, in general, $A(t)$ is not proportional to A_0. After two oscillations the amplitudes are of the same order, $A(t = 140) \simeq 6$, even though the initial amplitudes differ by a factor two. We confirm the following rule, already stated in ref. [8]: oscillations of initial amplitude A_0 much larger than $\Lambda/10$ decay rapidly, in one or two oscillations, till $A(t) \lesssim \Lambda/10$. After that the string is more weakly damped.

Fig. 8 shows $N_{ax}(t)$ for $A_0 = 30$, 20, 10 on a 256*256*64 lattice and $\lambda = 0.2$. N_{ax} increases slightly, of order 1%, and then oscillates about an average value. It is not clear to us whether this slight increase of N_{ax} is a real effect because we were unable to satisfy ourselves that it happens in the infinite volume limit. However, let us analyze it as a real effect. To this end, we need a formula for r in the case of bent strings, when only part of the string decays into axions. The fraction of string that has decayed between the initial time t_{in} and the final time t_{fin} is given by the fractional change $1 - \frac{\ell_{fin}}{\ell_{in}}$ in the length ℓ of the string between those times. For a sinusoidally shaped string the length is determined in terms of the amplitude A by

$$\ell = \int_0^{L_z} dz \sqrt{1 + (\frac{2\pi A}{\Lambda} \cos \frac{2\pi z}{\Lambda})^2} \quad . \tag{4.2}$$

Let us call N'_{ax} the value of N_{ax} restricted to that fraction of string which decays into axions between times t_{in} and t_{fin}. We have

$$N'_{ax}(t_{in}) = (1 - \frac{\ell_{fin}}{\ell_{in}})N_{ax}(t_{in}) \tag{4.3}$$

and

$$N'_{ax}(t_{fin}) = N_{ax}(t_{fin}) - \frac{\ell_{fin}}{\ell_{in}}N_{ax}(t_{in}) \quad . \tag{4.4}$$

Hence, we estimate r for bent string simulations using the formula

$$r = \frac{N'_{ax}(t_{fin})}{N'_{ax}(t_{in})} = \frac{N_{ax}(t_{fin}) - \frac{\ell_{fin}}{\ell_{in}}N_{ax}(t_{in})}{(1 - \frac{\ell_{fin}}{\ell_{in}})N_{ax}(t_{in})} \quad . \tag{4.5}$$

Table 1 shows the r values for $A_0 = 30$, 20, 10 and $\lambda = 0.05$, 0.1, 0.2 on a 256*256*64 lattice. r increases with decreasing A_0, reaching values of order 1.12 for $A_0 = 10$. However, for such small initial amplitudes, only a very small part of the energy stored in the string gets released. The larger amplitude ($A_0 \sim 0.5\Lambda$) simulations are more relevant because they are typical of the cosmological setting and because proportionately more energy gets released in them. For large initial amplitude, r is close to one and has a tendency to decrease with increasing $\ln(\frac{L}{\delta})$. In contrast, scenario A predicts that r is of order $\ln(\frac{L}{\delta})$.

12

V. VORTEX-ANTIVORTEX ANNIHILATION

We also studied the annihilation of vortex-antivortex pairs in 2D. The Lagrangian is the same as before, Eq. (1.2). Note however that in 2D the field ϕ and its expectation value v_a have dimension of (length)$^{-1/2}$, and λ has dimension of (length)$^{-1}$. The energy stored in a vortex at rest is $E \simeq \pi v_a^2 \ln(L/\delta)$, which is analogous to Eq.(1.5). The core size is $\delta = \frac{1}{\sqrt{\lambda} v_a}$ as before. For a vortex-antivortex pair, the distance R between them is the infra-red cutoff L. The total energy in the pair is therefore

$$E(R) \simeq 2\pi v_a^2 \ln(\frac{R}{\delta}) \tag{5.1}$$

when the vortex and antivortex are at rest.

A vortex-antivortex pair has zero topological charge. It annihilates by emitting Nambu-Goldstone (NG) radiation. We may think of this process in 3D as the annihilation of an infinitely long straight string with an infinitely long parallel antistring. This is not directly relevant to the problem considered here since long parallel axion strings are unlikely in the early universe. However, because it is 2D, the process can be accurately simulated. Moreover the behaviour of this relatively simple system can be predicted on theoretical grounds. We will argue below that the energy spectrum of NG radiation emitted by a spinning vortex anti-vortex pair has the qualitative shape $\frac{dE}{dk} \sim \frac{1}{k}$.

Simulations of vortex-antivortex annihilation were carried out previously in Refs. [19,25]. However, as far as we know, the present work is the first to spectrum analyze the NG radiation emitted in the decay. Ref. [26] presents simulations of the formation and evolution of vortices in an expanding 2+1 dimensional universe.

What should one expect the radiation spectrum to be? It is known that, in 2+1 dimensions, the axion field is dual to a gauge field which couples to the vortex as if it were a particle with electric charge $e = \sqrt{2\pi} v_a$. This is the restriction to 2+1 dimensions of the well-known duality [27,28,25] relating the axion field in 3+1 dimensions to an anti-symmetric two-index gauge field $A_{\mu\nu}(x)$ which couples to the world-sheet of the axion string. Hence, as long as the vortex and anti-vortex are at greater distance from one another than the sum of their core sizes ($R > 2\delta$), they behave like a pair of oppositely charged particles. When the cores of the vortex and anti-vortex start to overlap, this description is no longer valid. However, in the generic situation where the pair has angular momentum, most of the energy has already been dissipated into radiation by then.

The force between the vortex and anti-vortex is attractive and has magnitude

$$F(R) = \frac{2\pi v_a^2}{R} \quad . \tag{5.2}$$

It is a manifestation of the aforementioned duality that this force can be thought of either as the gradient of the potential energy (5.1) or as the Coulomb force between two oppositely charged particles, of charges $\pm\sqrt{2\pi} v_a$. The acceleration of both vortex and antivortex is therefore:

$$a \simeq \frac{2}{R \ln(\frac{R}{\delta})} \tag{5.3}$$

in the not highly relativistic regime, and neglecting the radiation reaction due to the emission of NG particles. The typical angular frequency of the radiation is $\omega \sim a \sim \frac{1}{R}$. Hence its spectrum has the generic form:

$$\frac{dE}{d\omega} = \frac{dE}{dR}\frac{dR}{d\omega} \sim 2\pi v_a^2 \frac{1}{R}\frac{1}{\omega^2} \sim 2\pi v_a^2 \frac{1}{\omega} \quad , \tag{5.4}$$

i.e. it is flat on a logarithmic scale. The low frequency radiation is emitted first and the high frequency last.

A 2048^2 lattice was initialized with the ansatz

$$\phi(x,y) = \phi_0(x - x_1, y - y_1)\, \phi_0^*(x - x_2, y - y_2) \tag{5.5}$$

where (x_1, y_1) and (x_2, y_2) are the locations of the vortex and antivortex respectively, and $\phi_0(x,y)$ is the field of a single vortex at rest. A relaxation routine was applied to this configuration with the cores held fixed. Periodic boundary conditions were used during the relaxation and the subsequent dynamical evolution. The vortex and antivortex were given an initial relative velocity v_0 perpendicular to their line of sight. The range of parameters simulated was $0 < v_0 < 0.6$ for the initial velocity and $5 < \delta < 30$ for the core size. Fig. 9 shows snapshots of a decaying vortex-antivortex system for $\lambda = 0.005$ and $v_0 = 0.5$. The initial and final $\frac{dE}{d\ln k}$ energy spectra are shown in Fig. 10. The initial spectrum, that of the initial vortex-antivortex pair, is flat like that of an axion string. The final spectrum is that of the NG radiation after the vortex and antivortex annihilated. It is also flat qualitatively, in agreement with the theoretical argument given above. In all cases, the final spectrum is found to be somewhat harder than the initial spectrum. Thus, N_{ax} decreases ($r < 1$) for all parameters investigated.

VI. CONCLUSIONS

We carried out numerical simulations of the decay of axion string into axions, for a variety of initial configurations. Our main goal is to estimate the factor $\bar{r}$ which appears in the expression for the axion cosmological energy density, Eq. (2.13). r is the relative increase of N_{ax} during a decay process. $\bar{r}$ is the average of r over the various processes that contribute. We simulated circular loops, non-circular loops and bent strings.

The circular loop simulations were done in 2D, exploiting the axial symmetry. This allowed us to reach $\ln(\frac{R_0}{\delta}) \simeq 5$. We found that circular loops collapse in one go, except in the range $80 < R_0/\delta < 190$ where they bounce once. As far as we know, the bounce phenomenon was not observed in previous simulations nor was it anticipated in theoretical investigations. We found $r \simeq 0.8$ for circular loops, whether or not they bounce. We did not find any dependence of r on $\ln(\frac{R_0}{\delta})$ over the range, $3.6 < \ln(\frac{R_0}{\delta}) < 5.0$, of the simulations. Our results are consistent with the previous simulations of circular loops in 3D by two of us [8], which showed $r \simeq 0.8$ over the range $2.6 < \ln(\frac{R_0}{\delta}) < 3.2$.

Twenty-one non-circular loop simulations were carried out using as initial conditions a family of Kibble-Turok configurations parametrized by α and ψ. In the case of Nambu-Goto strings, such initial conditions yield periodic non self-intersecting motion for most of the parameter space. In the simulations, the loops collapse in one go, without oscillation or

14

bounce. N_{ax} decreases in almost all cases. r depends on α, ψ and $\ln(\frac{R_0}{\delta})$, and ranged from 0.60 to 1.07. r decreases with increasing $\ln(\frac{R_0}{\delta})$ but appears to be reaching a limiting value for $\ln(\frac{R_0}{\delta}) \sim 3$. Nine simulations were done for $\ln(\frac{R_0}{\delta}) = 2.78$. The average of r over this set is 0.77.

The bent string simulations were done on lattices of size 256*256*64 and 256*256*128 with the string in the direction of the shortest dimension. We found that oscillations of initial amplitude A_0 much larger than $\Lambda/10$, where Λ is the wavelength of the wiggle, decay rapidly, in one or two oscillations, till $A(t) \lesssim \Lambda/10$. After that, the string is more weakly damped. This is consistent with what was found in ref. [8]. We find that N_{ax} increases slightly, by an amount of order 1%. The r values are listed in Table 1 for a representative set of parameter values.

Our simulations are inconsistent with scenario A which predicts that r is of order $\ln(\frac{L}{\delta})$. We find that r is of order one and also that r does not increase with increasing $\ln(\frac{L}{\delta})$ over the range investigated, $3 < \ln(\frac{L}{\delta}) < 5$. Our bent string simulations are also inconsistent with scenario A in that $A(t)$ is not proportional to the initial amplitude A_0.

Battye and Shellard [9] have carried out bent string simulations. Their string configuration is similar to ours. They conclude that the string emits radiation mainly at twice the oscillation frequency of the string and that the spectrum falls off exponentially for large k. We do not find evidence of this. To obtain the spectrum of radiated axions they subtract the field of a static straight string when the string is going through the equilibrium position. The subtracted field is assumed to be that of the radiated axions and is spectrum analyzed. It is unclear to us that this subtraction procedure is valid because it neglects retardation and Lorentz contraction effects associated with the fact that the string is moving when it is going through its equilibrium position.

Yamaguchi, Kawasaki and Yokoyama [11] carried out simulations of a network of global strings in an expanding universe. They found $\xi \simeq 1$ for the parameter which describes the average density of strings [Eq. (2.1)]. We use their result below. They find that the spectrum of radiated axions is softer than the $\frac{dE}{dk} \sim \frac{1}{k}$ spectrum of the energy stored in strings, whereas we find in most cases that it is somewhat harder. It must be kept in mind however that, because the Yamaguchi et al. simulations describe a network of many strings, their effective value of $\ln(\frac{L}{\delta})$ is small compared to the range of $\ln(\frac{L}{\delta})$ values explored by the simulations described here.

To estimate the axion cosmological energy density, we use $\bar{r} \simeq 0.8$ as implied by our circular and non-circular loop simulations. The contribution of bent long strings is expected to be much less important than that from closed loops. We use $\xi \simeq 1$ based on the simulations of global string networks in an expanding universe by Yamaguchi et al. [11], and set $N_d = 1$ and $\chi = 2^{\pm 1}$ as discussed in the Introduction. Hence our estimate for the string decay contribution:

$$\Omega_a^{\mathrm{str}} \simeq \frac{\xi \bar{r}}{\chi} \Omega_a^{\mathrm{vac}} \simeq 0.27 \ 2^{\pm 1} \left(\frac{f_a}{10^{12} \mathrm{GeV}} \right)^{\frac{7}{6}} \left(\frac{0.7}{h} \right)^2 \ . \tag{6.1}$$

For the reasons mentioned in the Introduction, the wall decay contribution is probably subdominant compared to the vacuum realignement and string decay contributions. Hence our estimate for the total density in cold axions today:

$$\Omega_a \simeq \Omega_a^{\text{vac}} + \Omega_a^{\text{str}} = (0.4 \text{ to } 0.9) \left(\frac{f_a}{10^{12}\text{GeV}} \right)^{\frac{7}{6}} \left(\frac{0.7}{h} \right)^2 \quad . \tag{6.2}$$

This is relevant to the dark matter searches presently in progress [30,31], insofar that it suggests the range of axion masses for which axions are the dark matter of the universe. Let us remind the reader that the above estimate is for the case where there is no inflation after the PQ phase transition. It also assumes that the axion to entropy ratio is constant from time t_1 till the present. Various ways in which this assumption may be violated are discussed in the papers of ref. [32].

Finally, we simulated the annihilation of vortex-antivortex pairs in 2D. We find that the spectrum of radiated axions has the qualitative shape $\frac{dE}{dk} \sim \frac{1}{k}$. This is consistent with our theoretical analysis of the system. We find that N_{ax} decreases in this case too.

ACKNOWLEDGMENTS

REFERENCES

[1] S. Weinberg, Phys. Rev. Lett. 40, 223 (1978); F. Wilczek, Phys. Rev. Lett. 40, 279 (1978).

[2] R. Peccei and H. Quinn, Phys. Rev. Lett. 38, 1440 (1977), and Phys. Rev. D16, 1791 (1977).

[3] J.E. Kim, Phys. Rep. 150, 1 (1987); H.-Y. Cheng, Phys. Rep. 158, 1 (1988); M.S. Turner, Phys. Rep. 197, 67 (1990); G.G. Raffelt, Phys. Rep. 198, 1 (1990).

[4] L. Abbott and P. Sikivie, Phys. Lett. B120, 133 (1983); J. Preskill, M. Wise and F. Wilczek, Phys. Lett. B120 127 (1983); M. Dine and W. Fischler, Phys. Lett. B120, 137 (1983).

[5] R. Davis, Phys. Rev. D32, 3172 (1985); Phys. Lett. 180B, 225 (1985).

[6] D. Harari and P. Sikivie, Phys. Lett. B195, 361 (1987).

[7] R.L. Davis and E.P.S. Shellard, Nucl. Phys. B324, 167 (1989).

[8] C. Hagmann and P. Sikivie, Nucl. Phys. B363, 247 (1991).

[9] R.A. Battye and E.P.S. Shellard, Phys. Rev. Lett. 73, 2954 (1994); (E) ibid. 76, 2203 (1996).

[10] C. Hagmann, S. Chang and P. Sikivie, Nucl. Phys. B Proc. Suppl. 72, 81 (1999).

[11] M. Yamaguchi, M. Kawasaki and J. Yokoyama, Phys. Rev. Lett. 82, 4578 (1999).

[12] D. Lyth, Phys. Lett. B275, 279 (1992).

[13] M. Nagasawa and M. Kawasaki, Phys. Rev. D50, 4821 (1994).

[14] S. Chang, C. Hagmann, and P. Sikivie, Phys. Rev. D59, 023505 (1999).

[15] A.P. Zhitnitskii, Sov. J. Nucl. Phys. 31, 260 (1980); M. Dine, W. Fischler and M. Srednicki, Phys. Lett. B104, 199 (1981).

[16] J. Kim, Phys. Rev. Lett. 43, 103 (1979); M.A. Shifman, A.I. Vainshtein and V.I. Zakharov, Nucl. Phys. B166, 493 (1980).

[17] P. Sikivie, Phys. Rev. Lett. 48, 1156 (1982).

[18] A. Vilenkin and A.E. Everett, Phys. Rev. Lett. 48, 1867 (1982); P. Sikivie in *Where are the Elementary Particles*, Proc. of the 14th Summer School on Particle Physics, Gif-sur-Yvette, 1982, edited by P. Fayet et al., Inst. Nat. Phys. Nucl. Phys. Particules, Paris, 1983.

[19] E.P.S. Shellard, Nucl. Phys. B283, 624 (1987).

[20] P. Goddard, J. Goldstone, C. Rebbi and C.B. Thorn, Nucl. Phys. **B56** 109 (1973).

[21] T.W.B. Kibble and N. Turok, Phys. Lett. 116B, 141 (1982).

[22] N. Turok, Nucl. Phys. B242, 520 (1984).

[23] C. Burden, Phys. Lett. 164B, 277 (1985).

[24] A.L. Chen, D.A. DiCarlo, and S.A. Hotes, Phys. Rev. D37, 863 (1988).

[25] M. Hecht and T. DeGrand, Phys. Rev. D42, 519 (1990).

[26] M. Yamaguchi, J. Yokoyama and M. Kawasaki, Prog. Theor. Phys. 100, 535 (1998).

[27] M. Kalb and P. Ramond, Phys. Rev. D9, 2273 (1974).

[28] E. Witten, Phys. Lett. B158, 243 (1985).

[29] R.A. Battye and E.P.S. Shellard, Nucl. Phys. B Proc. Suppl. 72, 88 (1999)

[30] C. Hagmann et al., Phys. Rev. Lett. 80, 2043 (1998); H. Peng et al., NIM A444, 569 (2000)

[31] S. Matsuki and K. Yamamoto, Phys. Lett. B263, 523 (1991); I. Ogawa, S. Matsuki and K. Yamamoto, Phys. Rev. D53, R1740 (1996).

[32] P. J. Steinhardt and M. S. Turner, Phys. Lett. B129, 51 (1983); W. G. Unruh and R. M. Wald, Phys. Rev. D32, 831 (1985); M. S. Turner, Phys. Rev. D32, 843 (1985); T. DeGrand, T. W. Kephart and T. J. Weiler, Phys. Rev. D33, 910 (1986); C. T. Hill and G. G. Ross, Nucl. Phys. B311, 253 (1988); G. Lazarides, R. Schaefer, D. Seckel and Q. Shafi, Nucl. Phys. B346, 193 (1990); M. Hindmarsh, Phys. Rev. D45, 1130 (1992).

TABLES

TABLE I. r values for bent string simulations on a 256*256*64 lattice. We used $L = 64$ for estimating $\ln(\frac{L}{\delta})$.

λ	$\ln(\frac{L}{\delta})$	A_0	r
0.05	2.7	30	1.07
0.05	2.7	20	1.08
0.05	2.7	10	1.12
0.1	3.0	30	1.04
0.1	3.0	20	1.06
0.1	3.0	10	1.12
0.2	3.4	30	1.02
0.2	3.4	20	1.05
0.2	3.4	10	1.12
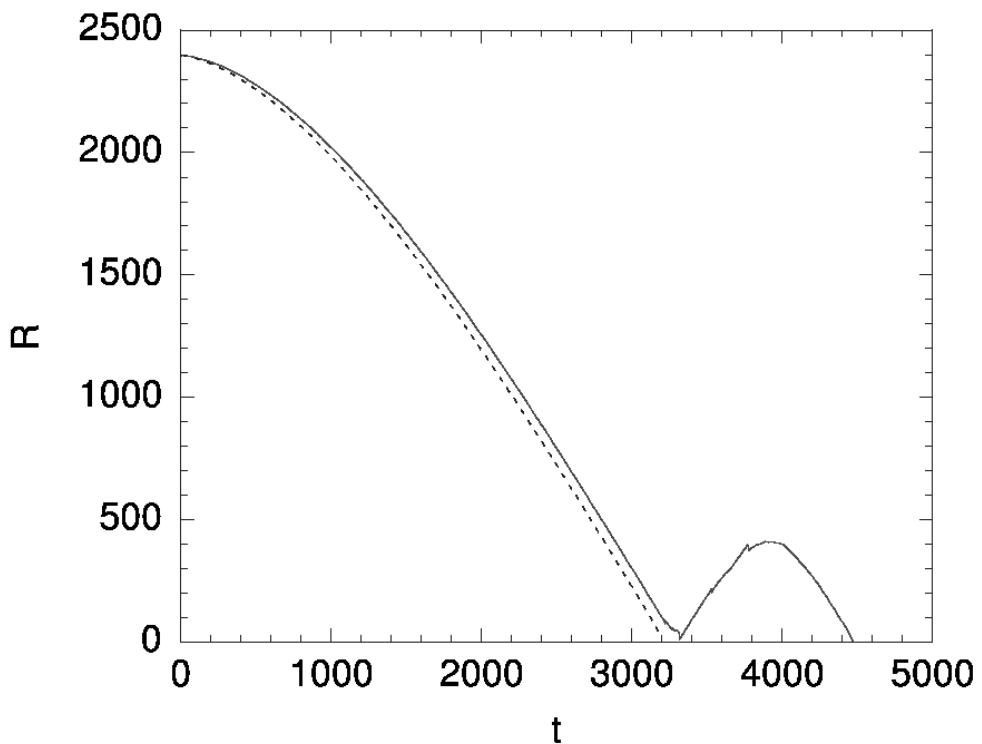
FIG. 1. Radius versus time of a collapsing circular loop, for $\lambda = 0.001$ (dotted line) and $\lambda = 0.004$ (solid line).
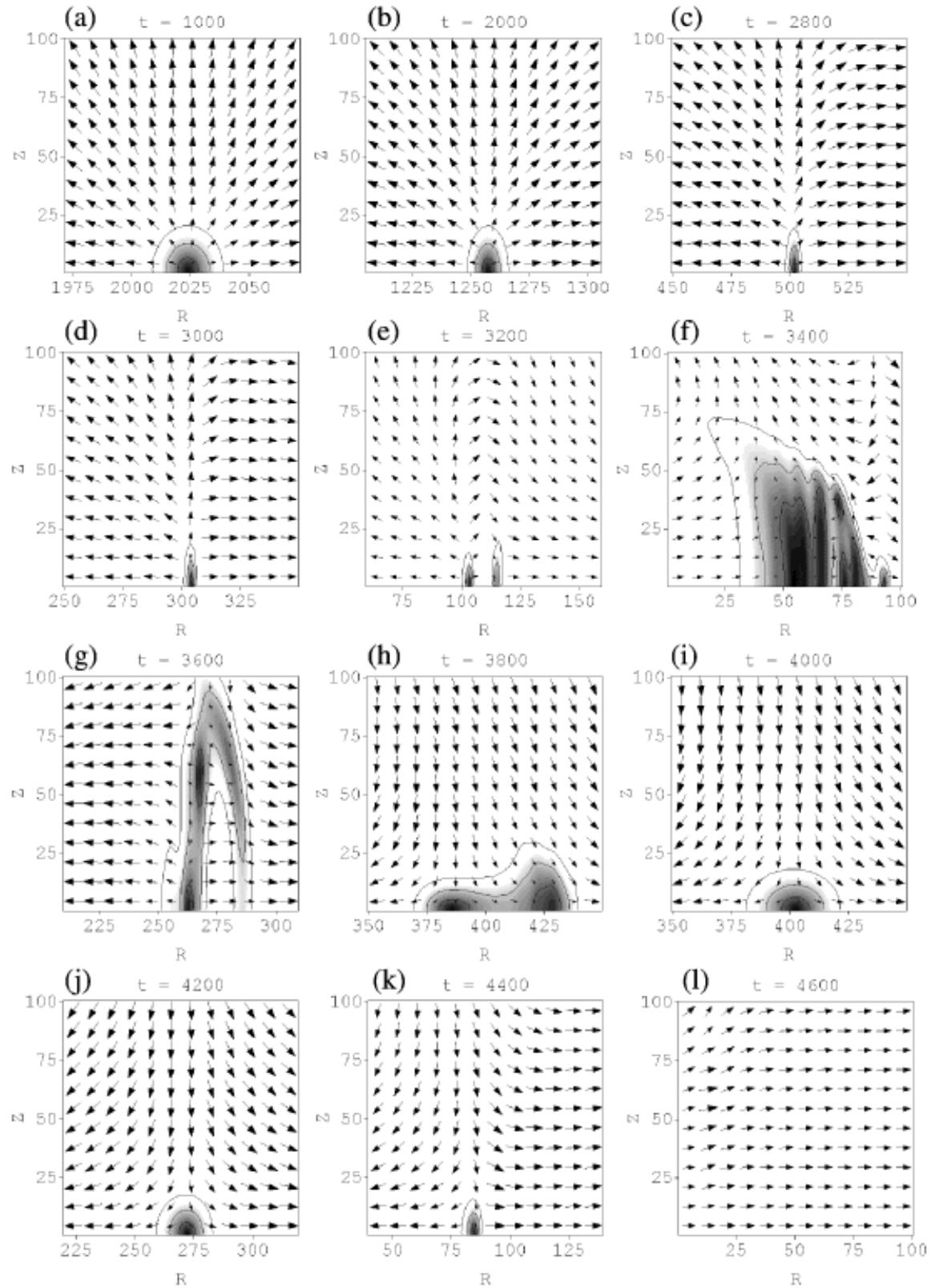
FIG. 2. Snapshots of a collapsing circular loop. The arrows give the direction of (ϕ_1, ϕ_2) in internal space. The grey-scale shows the magnitude of $|\phi|$, white for $|\phi| = 1$ and black for $|\phi| = 0$.

21
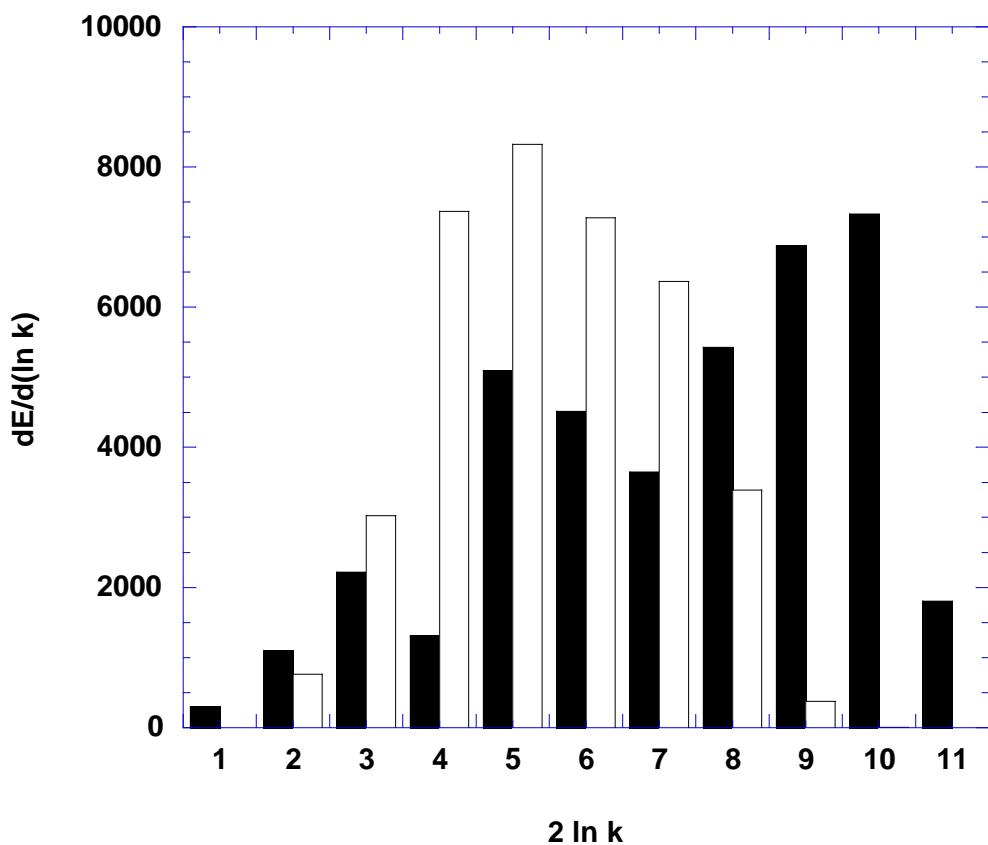
FIG. 3. Spectrum of decaying circular loop for $R_0 = 2400$, $\lambda = 0.004$, at times $t = 0$ (open boxes) and $t = 5000$ (closed boxes).
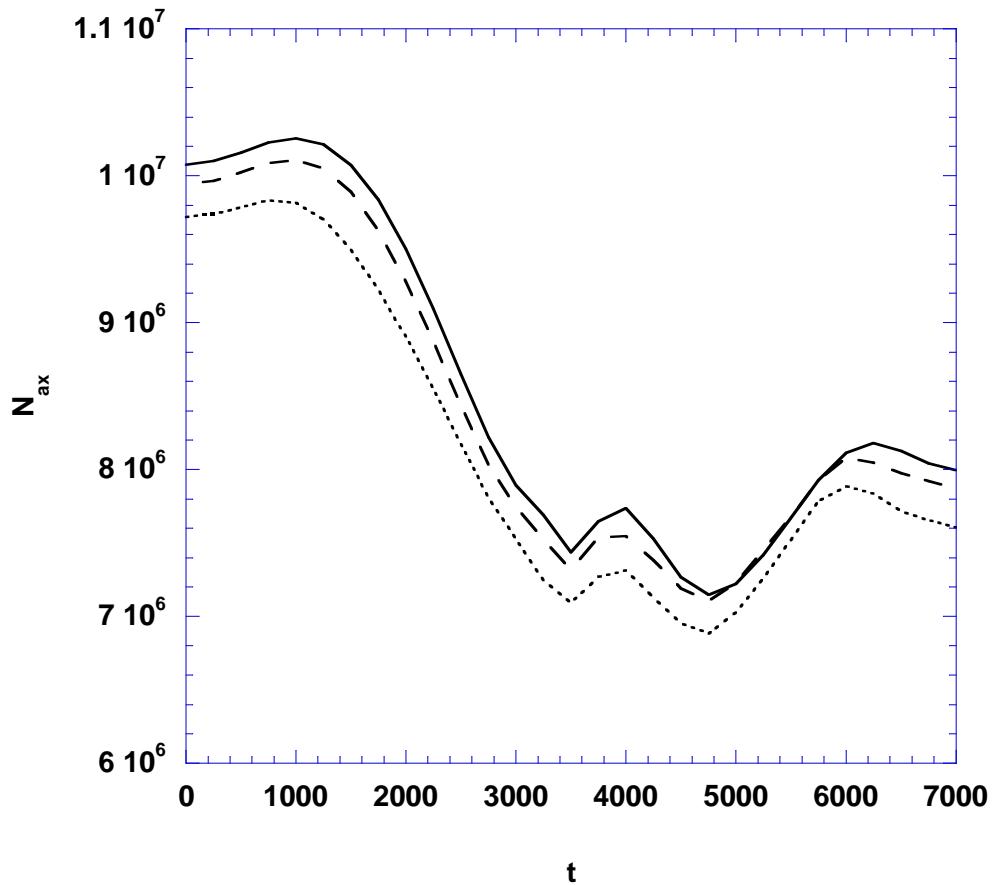
FIG. 4. N_{ax} versus time of a circular loop for $R_0 = 2400$, $L_\rho = 4000$, $L_z = 4096$ and $\lambda = 0.004$ (solid), 0.001 (dashed), and 0.00025 (dotted).
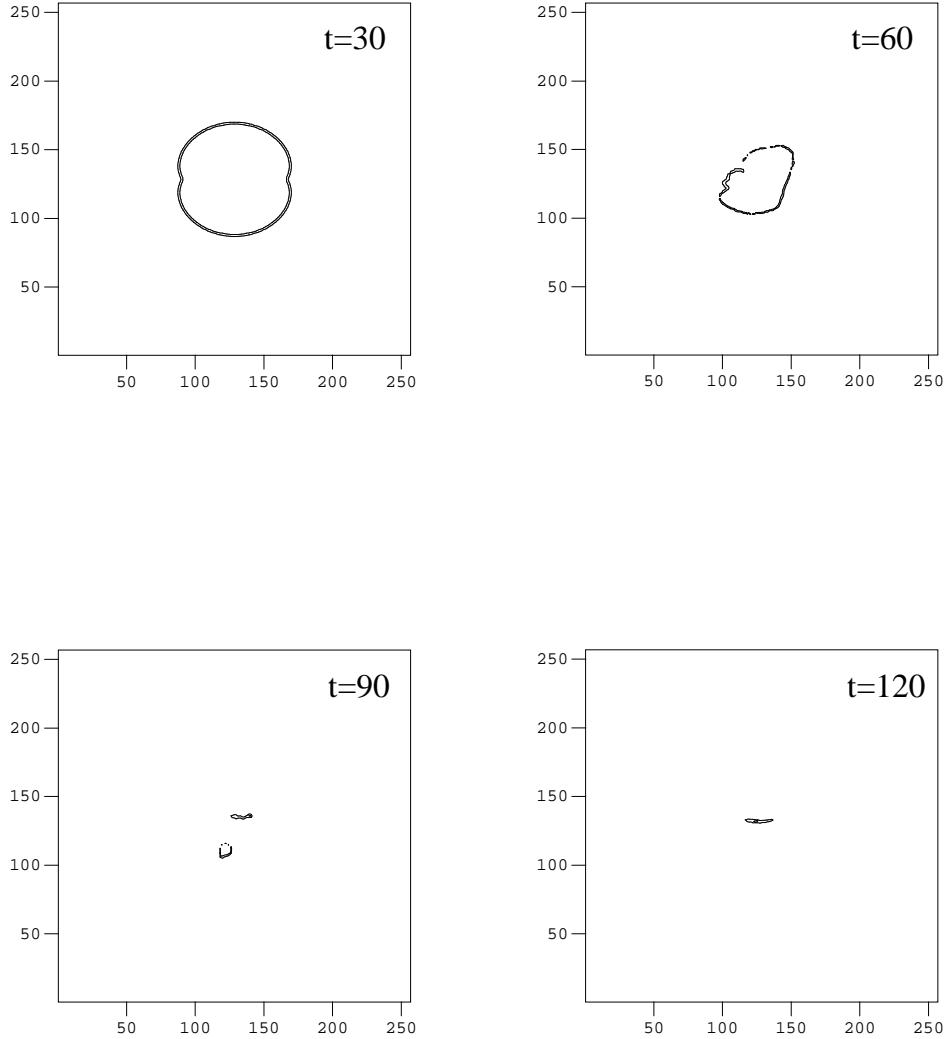
FIG. 5. Snapshots of a collapsing non-circular loop. The simulation is carried out on a 256^3 lattice with $\lambda = 0.05$. The initial conditions are given by Eq. (3.7) with $\alpha = 0.7, \psi = \pi/2, R_0 = 72$. The position of the string core is projeced onto the xz plane.
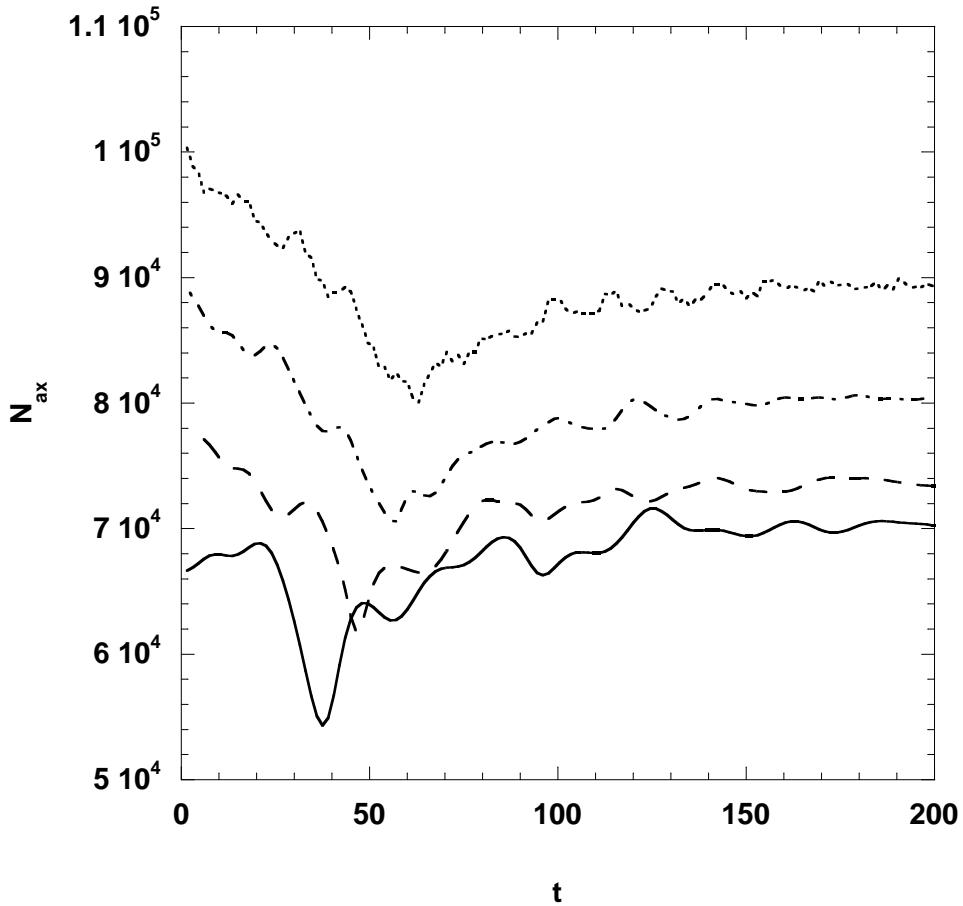
FIG. 6. N_{ax} versus time for four non-circular loop simulations on a 256^3 lattice. The initial conditions are given by Eq. (3.7) with $R_0 = 72, \alpha = 0.3, \psi = \pi/2$, and $\lambda = 0.1$ (dotted), 0.05 (dot-dashed), 0.025 (dashed) and 0.0125 (solid).

25
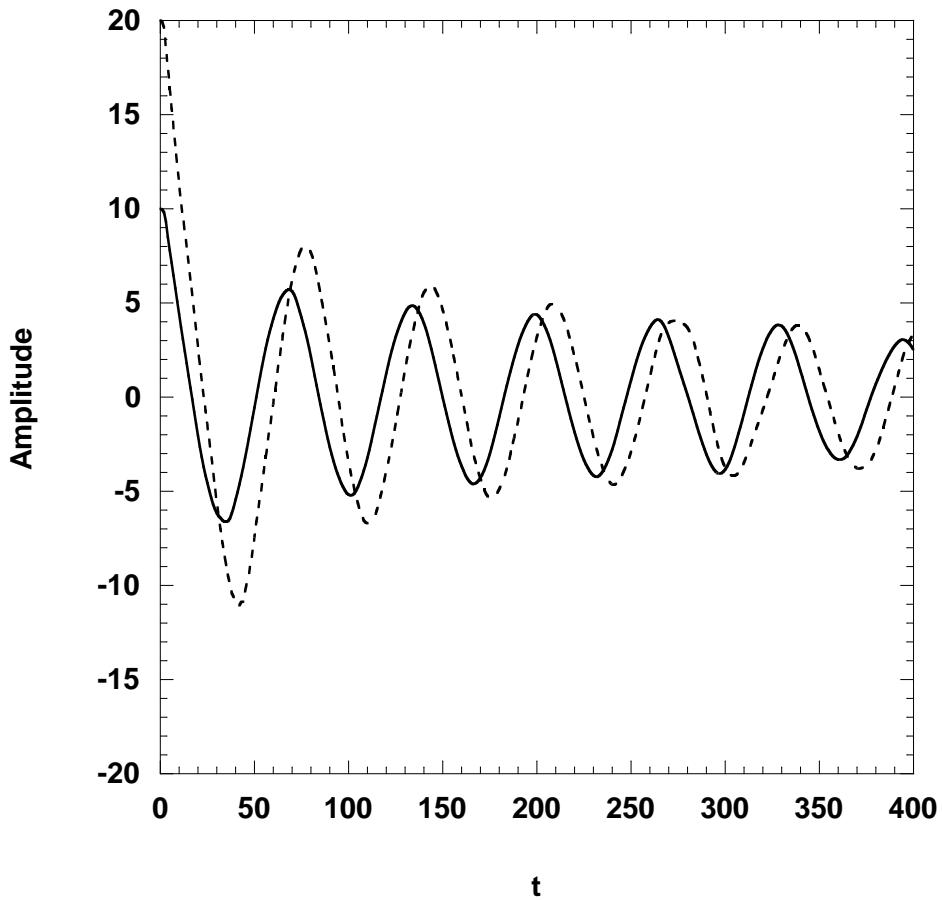
FIG. 7. String core position of oscillating bent strings versus time. The simulation is carried out on a $L_x L_y L_z = 256^2 * 64$ lattice with $\Lambda = 64$, $\lambda = 0.2$, and $A_0 = 20$ and 10.
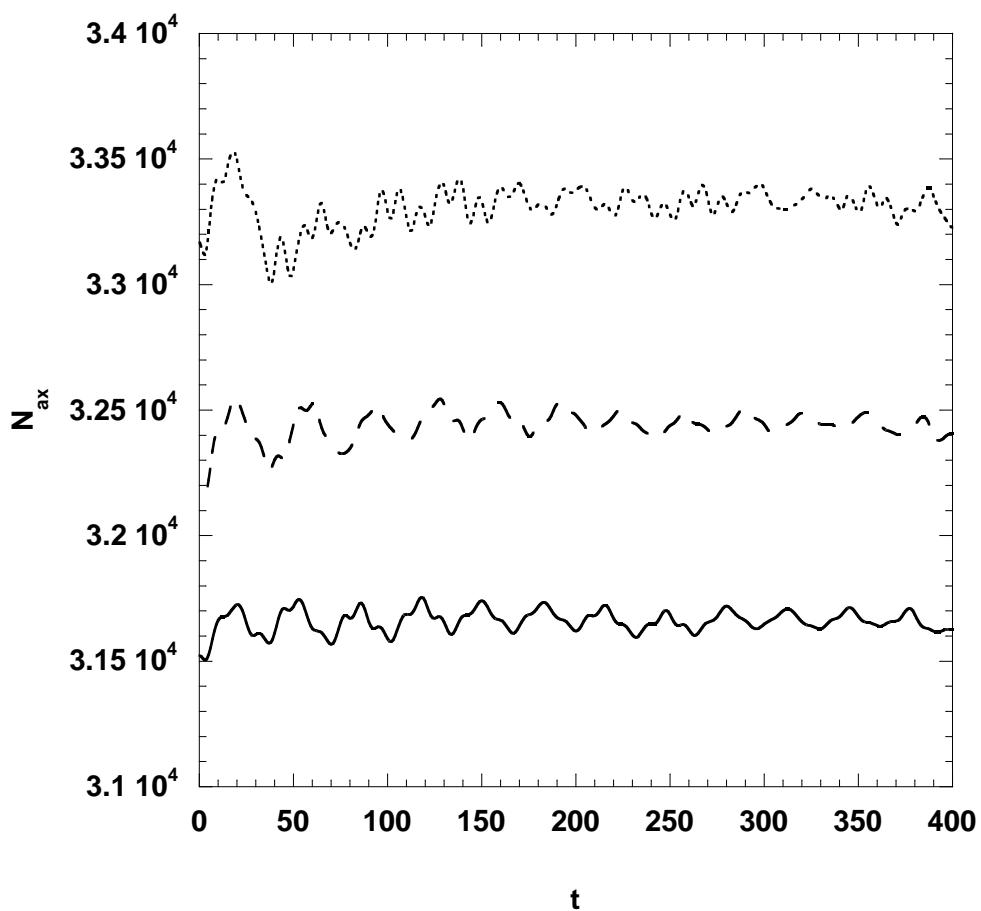
FIG. 8. N_{ax} for an oscillating bent string versus time. Here $L_x L_y L_z = 256^2 * 64$, $\Lambda = 64$, $\lambda = 0.2$ and $A_0 = 30$(dotted), 20(dashed), 10(solid)

.
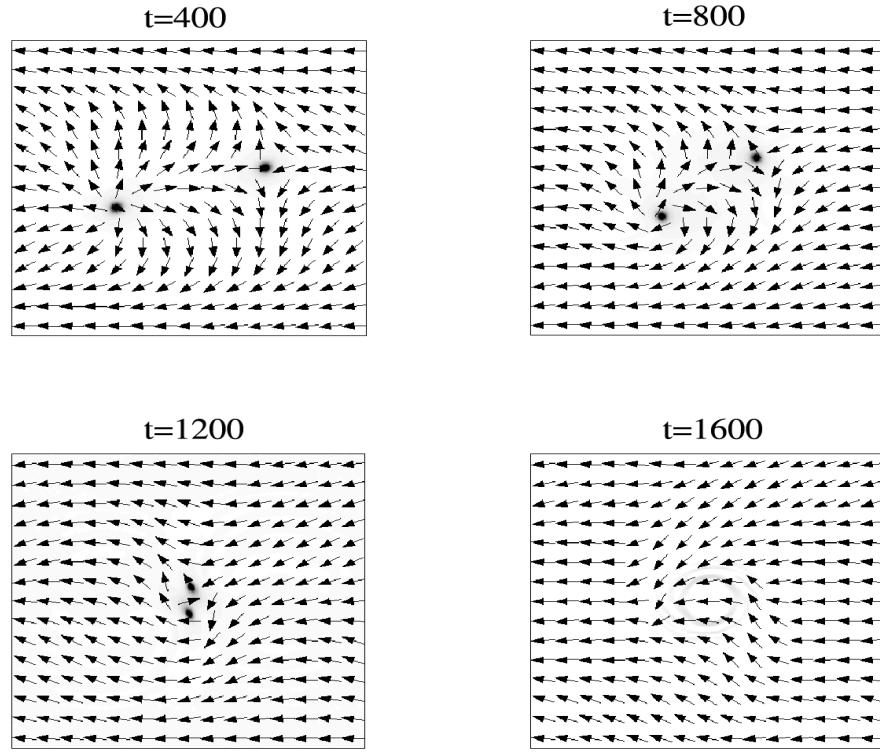
FIG. 9. Snapshots of collapsing vortex-antivortex pairs. The simulation is carried out on a 2048^2 lattice with $\lambda = 0.005$ and $v_0 = 0.5$. The initial separation between the vortex and anti-vortex is 1000 lattice units.
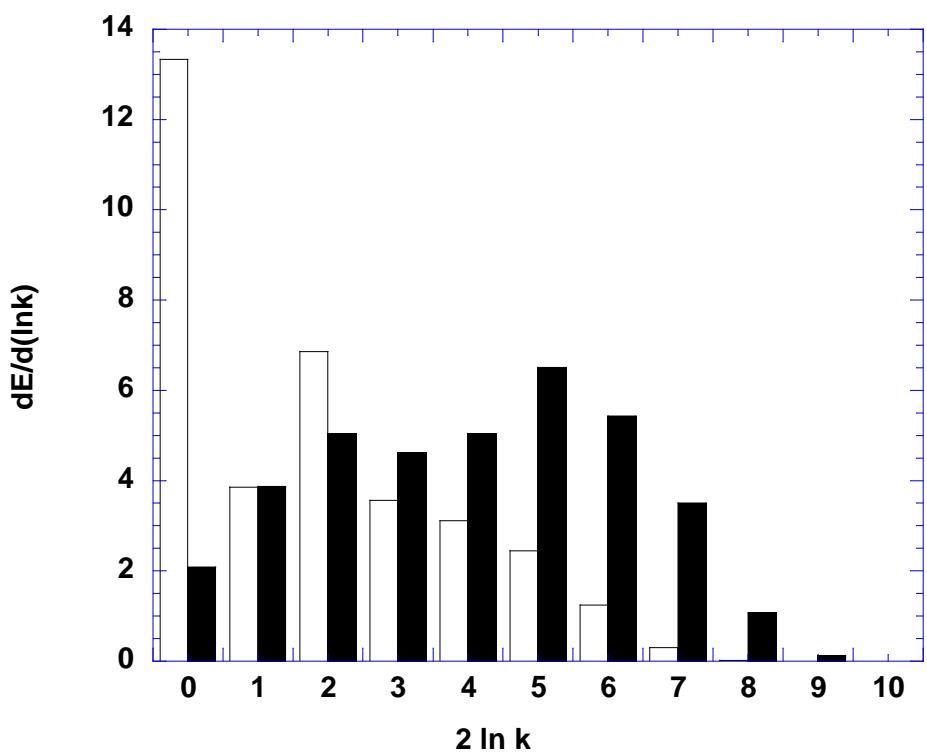
FIG. 10. Spectra of a vortex-antivortex pair at time times $t = 0$ (open boxes) and $t = 2000$ (closed boxes). The parameter values are the same as in Fig. 9.